A Carbon-13 NMR Study of the Phase Structure of Semicrystalline Polymers: Hydrogenated Polybutadiene

R. Kitamaru*,† and T. Nakaoki

Science and Technology, Ryukoku University, Seta Otsu 520, Japan

R. G. Alamo‡ and L. Mandelkern

Department of Chemistry and Institute of Molecular Biophysics, Florida State University, Tallahassee, Florida 32306-3015

Received November 20, 1995; Revised Manuscript Received May 20, 1996⊗

ABSTRACT: A carbon-13 solid-state NMR study was made of a set of model random ethylene copolymers, namely the hydrogenated polybutadienes. By adopting appropriate pulsing sequences, the different elements of phase structure were isolated and the characteristics of the crystalline, amorphous, and crystalline−amorphous interfacial regions were established. The relative amounts and the thicknesses were determined for each of these regions. The results obtained by the NMR method agree very favorably with those previously reported by Raman spectroscopy with identical copolymers.

Introduction

In 1949 Flory pointed out that because of conformational restraints, the boundary between the crystalline and amorphous regions of most long-chain molecules will not be sharply defined as is typical of monomeric systems.[1] Subsequent theoretical analyses, involving several different methods, have quantitatively established the existence of a diffuse interfacial region between the two phases.[2−11] Over the past few years, a variety of experimental methods have confirmed the expectation of such an interphase.[12] These methods involve ^{13}C solid-state NMR,[13−16] Raman spectroscopy,[17−19] and small-angle X-ray and neutron scattering among others.[20−26] In general, good agreement has been obtained between the different methods for both the relative amount and the thickness of the interfacial region.[1,26]

The detailed phase structure of linear polyethylene,[13] isotactic polypropylene,[14] and poly(tetramethylene oxide)[15] has been previously studied using high-resolution ^{13}C solid-state NMR. The existence of the crystalline−amorphous interphase in these polymers was confirmed by these works. These investigators were also able to characterize the interphase as well as the crystalline and noncrystalline amorphous phases as defined regions that differ in their chemical shifts and relaxation times. Put another way, these three phases differ in molecular chain conformation and dynamics. In the present work, we extend this NMR method to a study of the phase structure of the model random copolymer, hydrogenated polybutadiene. This sample, which can be considered to be an ethylene-*co*-butene copolymer, has a very narrow molecular weight and composition distribution, and the co-units are randomly distributed. We will focus our primary attention here on the existence and properties of the crystal−amorphous interphase and compare our results with those obtained by other methods that have studied the same type of copolymer.

† Present address: 11 Hanazono Enjyoji, Ukyo, Kyoto 616, Japan.

‡ Present address: Department of Chemical Engineering, FAMU/FSU College of Engineering, 2525 Pottsdamer St., Tallahassee, FL 32310-6046.

⊗ Abstract published in *Advance ACS Abstracts,* September 15, 1996.

Experimental Section

Samples. Two hydrogenated polybutadiene samples (linear polyethylene with randomly distributed ethyl branches) having molecular weights of 16 000 and 420 000 were used. These samples were crystallized by quenching the sample from the melt to −78 °C. The concentration of ethyl branches in both samples was found to be 2.2 mol % (22 branches per 1000 main-chain methylene carbons) using standard high-resolution ^{13}C NMR methods.[27−29] The characterization of these polymers by Raman spectroscopy, DSC, and small-angle X-ray methods is given in Table 1.[30]

^{13}C NMR. The ^{1}H dipolar decoupling/magic angle spinning (DD/MAS) ^{13}C NMR measurements were carried out at a field strength of 4.7 T with a Bruker MSL 200 spectrometer at room temperature. The ^{13}C resonance frequency was 50.3 MHz, and the B_1 strength used was 65 kHz for both ^{13}C and ^{1}H. The MAS was carried out at 4 kHz.

The pulse sequences used in this work are shown schematically in Figure 1. Pulse sequence I is the conventional single-pulse sequence for the solid-state ^{13}C NMR without cross-polarization (CP). If the repeating time of this sequence is greater than 5 times the spin−lattice relaxation time T_{1C}, the spectrum that is obtained will be in the thermal equilibrium state. It reflects accurately the contributions from all of the components in the system. After ensuring the complete recovery of the equilibrium magnetization, the magnetization was directed 90° perpendicular to the static field B_0 and the free induction decay (FID) was observed under ^{1}H dipolar decoupling. The Fourier transform of the FID gives the thermal equilibrium spectrum.

Pulse sequence II is a modified saturation−recovery pulse sequence. After saturating the magnetization by a 90° pulse train, the magnetization appearing in the B_0 direction for chosen times τ_1 was determined by observing the FID under ^{1}H dipolar decoupling. The Fourier transform of the FID provides the spectrum at each saturation−recovery step and the spin−lattice relaxation time T_{1C} of each resonance in the spectrum. The magnetization of the components with the shorter T_{1C}'s will appear first in this pulse sequence. The spectrum that is obtained in the early stages of the saturation−recovery (at the shorter τ_1's) will only reflect contributions from components with shorter T_{1C}'s.

Pulse sequence III is the combined pulse sequence of saturation−recovery and transverse relaxation. It is used to study the transverse relaxation phenomena of the different phases. In this case, the magnetization recovering in the B_0 direction for τ_1 was turned 90°. After allowing transverse relaxation for the time τ_t, the FID of the remaining magnetization in the direction perpendicular to B_0 was observed under ^{1}H decoupling. $^{1}H-^{13}C$ CP was not used in any of these three

S0024-9297(95)01724-4 CCC: $12.00

Table 1. Characterization of Hydrogenated Polybutadienes

			mass fraction and thickness							
			amorphous		interphase		crystalline			
	M_w	M_w/M_n	α_a[a]	L_a (Å)	α_b	L_b (Å)	α_c	L_c (Å)	crystallinity $(1-\lambda)_{\Delta H}$	spacing (SAXS) (Å)
P16	16000	1.40	0.51	90	0.12	10	0.37	53	0.40	144
P420	420000	1.84	0.68	115	0.13	10	0.17	27	0.22	145

[a] α_a, α_b, α_c and L_a, L_b, L_c denote, respectively, the mass fractions (α) and thicknesses (L) of the amorphous phase, interphase, and crystalline phase obtained from Raman spectroscopy. $(1-\lambda)_{\Delta H}$ denotes the degree of crystallinity determined by the enthalpy of fusion. Most of the data were taken from ref 30.

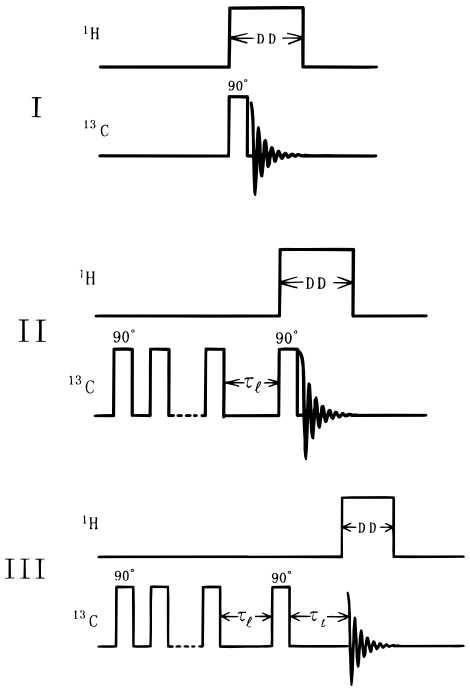

Figure 1. Schematic representation of the pulse sequences used in this work. Pulse sequence I is the conventional single-pulse sequence without CP for solid-state ^{13}C NMR. Pulse sequence II is the modified saturation−recovery pulse that is used to examine the longitudinal relaxation. Pulse sequence III is the combined pulse sequence of the saturation−recovery and the transverse relaxation. τ_1 and τ_t denote the time for the longitudinal and transversal relaxations, respectively. See text for details.

pulse sequences in order to avoid the complexity which can arise from different CP efficiencies of the different phases. The CP was used only for Torchia's pulse sequence (CPT1 pulse sequence)[31] in order to obtain the elementary lineshapes of the pure crystalline state.

Results and Discussion

Thermal Equilibrium Spectra. Figure 2 shows the DD/MAS ^{13}C NMR spectra obtained by using pulse sequence I $(2000\ s-\pi/2-FID)_n$ for the two samples. Since the repeating time of 2000 s that is used is greater than 5 times the longest T_{1C} for any of the phases, these spectra can be considered to be in the thermal equilibrium state. They, thus, contain all the contributions from the three phases. Two sharp resonance lines are observed at 32.4 and 30.5 ppm for tetramethylsilane (Me_4Si). These can be assigned to the methylene carbons in the orthorhombic crystalline and noncrystalline phases, respectively. The weak resonance at 10.8 ppm can be assigned to the methyl carbon ($1B_2$ carbon) of the ethyl branches. Although the spectra in Figure 2 reproduce the contributions from all of the phases, an examination of these spectra by themselves does not provide the detailed information of the phase structure that is wanted. Hence, it is necessary to examine the relaxation behavior before analyzing these spectra any further.

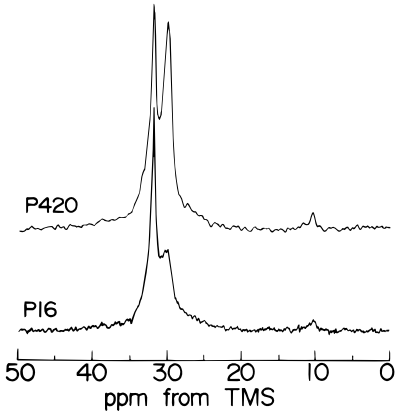

Figure 2. Thermal equilibrium spectra for the two hydrogenated polybutadiene samples P420 and P16. The spectra were obtained with a repetition time of 2000 s (2000 s−π/2−FID).

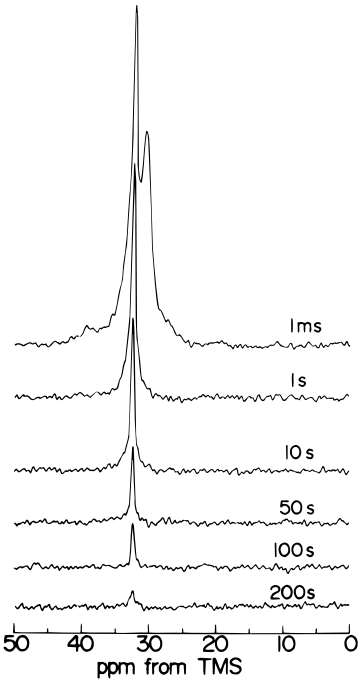

Figure 3. Partially relaxed spectra of sample P420 in the CPT1 pulse sequence. The longitudinal relaxation time is indicated in each spectrum.

We first analyze the longitudinal relaxation by use of the CPT1 pulse sequence in order to determine the elementary lineshape of the pure crystalline phase. Figure 3 gives the actual spectra obtained in the time progression of the CPT1 sequence for sample P420. In this sequence, the shorter T_{1C} contributions disappear first. The contributions from the longer T_{1C} phases persist at longer times. We find that within 1 s the

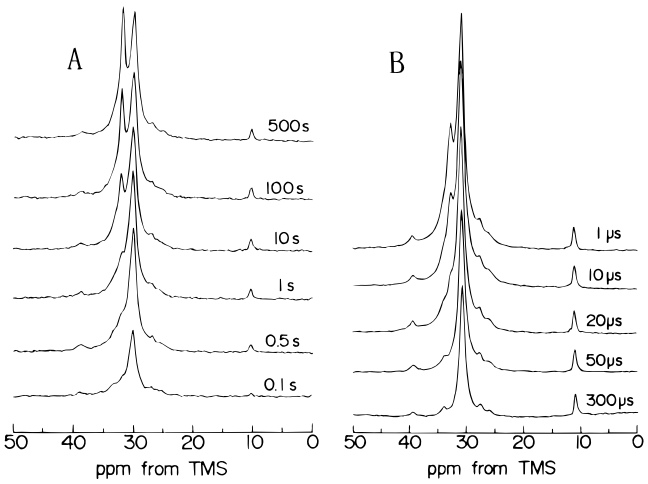

Figure 4. (A) Saturation−recovery spectra obtained with pulse sequence II for sample P420. τ_1 is indicated in each spectrum. (B) Transversely relaxed spectra obtained with pulse sequence III with $\tau_1 = 5$ s for sample P420. τ_t is indicated in each spectrum. Weak resonances assignable to the methine and methylene (α and β to the methine and methylene in the ethyl side group) carbons are observed at ca. 39, 34, 28, and 26 ppm. These are not discussed here.

noncrystalline contribution at ca. 30 ppm essentially disappears. Only the crystalline contribution remains over 200 s. The longest T_{1C} was estimated, by the modified saturation−recovery pulse sequence (sequence II), to be 82 s for the orthorhombic crystalline phase of this sample. This value of T_{1C} is comparable to that previously reported for polyethylenes of similar crystallite thickness.[16] The linewidth of the spectra for delay times greater than 50 s, where the only contribution is from the orthorhombic crystalline phase, is ca. 0.6 ppm. This value corresponds to ca. 30 Hz. This linewidth is somewhat larger than 18−20 Hz reported for the crystalline phase of linear polyethylene.[13] This relative broadening could be a result of the expanded lattice that is well known for this type of copolymer.[32,33]

Longitudinal and Transverse Relaxation Phenomena by Pulse Sequences II and III. We next examine the longitudinal and transverse relaxation behavior using sequences II and III in order to determine the noncrystalline content of these samples. Figures 4A and 4B show the actual time progression spectra obtained with sequences II and III, respectively, for sample P420. In Figure 4A the resonance centered at ca. 30 ppm, which is assigned to the noncrystalline main-chain methylene carbons, appears first. The 10.8 ppm line assignable to methyl carbons ($1B_2$ carbons) in ethyl branches also appears at this point. The crystalline resonance at 32.4 ppm, which has a longer spin−lattice relaxation time T_{1C}, appears later as the longitudinal recovery time τ_1 increases. After 500 s the shape of the spectrum approaches that of the equilibrium spectrum that was obtained by the single-pulse sequence and was illustrated in Figure 2. We note that only the noncrystalline contributions predominate in the spectra obtained in the interval at $\tau_1 = 0.1-1.0$ s.[34] It includes a downfield shoulder of the main noncrystalline resonance that is centered at 32.0 ppm. This observation indicates that the resonance of the noncrystalline component consists of two contributions that differ in their chemical shifts but have almost the same T_{1C} (0.16 s). This result implies that they differ in molecular conformation and distribution but have similar segmental mobilities in the T_{1C} relaxation time frame.

In order to analyze the proportion of the two noncrystalline components, we have examined the transverse relaxation (T_{2C} relaxation) of the noncrystalline resonance. The results are given in Figure 4B. Here the magnetization that was developed by the longitudinal recovery for τ_1 of 5 s was turned 90° and transverse relaxation was allowed for the chosen times τ_t. The FID was observed under ^{1}H decoupling. The spectrum at each τ_t increment was obtained from the Fourier transform of the FID. We note that the downfield shoulder at 32.0 ppm of the noncrystalline resonance disappears within 50 μs. However, the main noncrystalline resonance persists for over 300 μs at 30.5 ppm. This shows that the downfield shoulder and the main noncrystalline resonance are associated with very short and rather long T_{2C} values, respectively. The spin−spin relaxation time T_{2C} was estimated to be 24 and 410 μs for the downfield shoulder and the main noncrystalline resonance, respectively. We can thus conclude that there are two noncrystalline components. Their existence is demonstrated by the different chemical shifts and the distinctly different values for T_{2C}.

Since the two noncrystalline phases have different T_{2C}'s and a common T_{1C} of 0.16 s, these phases should involve plural motions described by different correlation times τ_c. As is well known, the spin relaxation due to the dipole−dipole interaction between ^{13}C and ^{1}H nuclei is described by the spectral densities. Here spectral density is defined as the Fourier transform of the correlation function of each term of the dipole interaction. In particular, T_{1C} is determined by the Larmor frequency components of ^{13}C and ^{1}H (ca. 10^8 Hz components in the present case), whereas as T_{2C} is determined by the zero-frequency component of the spectra density, because it dominates other larger frequency components for solid or viscous matter as in the present case. The fact that T_{1C} is the same indicates that relatively rapid motions with τ_c shorter than 10^{-8} s are the same for the two phases, because the spectral density at 10^8 Hz of slower motions with τ_c longer than 10^{-7} s is negligible in comparison to that of the rapid motions with τ_c shorter than 10^{-8} s. On the other hand, the different T_{2C}'s show different molecular motions in the two phases in slower motions accompanying a conformational change with regard to 10−20 carbon atoms.

The lineshapes for τ_t greater than 50 μs (Figure 4B), the T_{1C} value of 0.16 s, and the T_{2C} of 0.41 ms are typical of the rubbery state of polymers.[13] The main noncrystalline resonance thus represents the contribution from the liquid-like region with the associated random chain conformation and rubber-like mobility. In contrast, considering its broad lineshape as well as the T_{1C} and T_{2C} values, the downfield resonance reflects the contribution from the crystalline−amorphous interphase. The T_{1C} value of the interphase is the same as that of the liquid-like amorphous phase because it probes the more rapid segmental motion. In both cases, this involves disordered *gauche* and *trans* units. Thus, the T_{1C} of the interphase is similar to that of the amorphous phase but very different from that of the crystalline one. On the other hand, different relaxation behavior with regard to slower segmental motion will be expected between the conformationally disordered amorphous region and the partially ordered interphase. The segmental constraints over a dimension of 10−20 carbon atoms should be different between these two phases. This expectation is reflected in the different T_{2C} times.

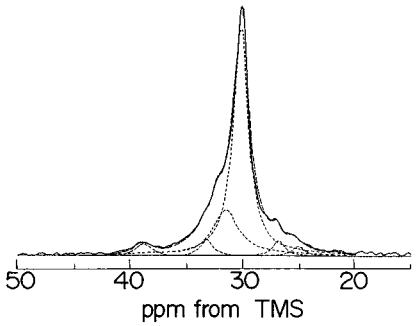

Figure 5. Lineshape analysis of the noncrystalline spectrum that was obtained using pulse sequence II with $\tau_1 = 0.5$ s for sample P420. The dotted curves at 30.5 and 32.0 ppm represent Lorentzians for the amorphous noncrystalline phase and the crystalline−amorphous interphase, respectively. The contributions from the resonances at 39, 34, 28, and 26 ppm that are assigned to the methine and methylene (α and β to the methine and methylene in the ethyl side group) carbons are also treated as Lorentzian lines as shown by the dotted curves. The dashed curve that is practically superposed on the experimental spectrum indicates the composite curve of the component Lorentzians.

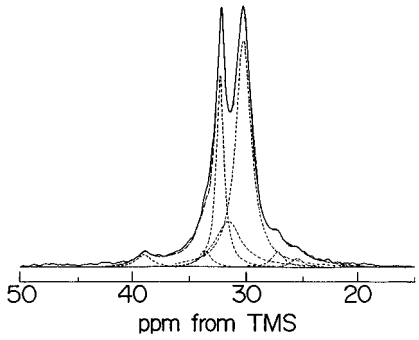

Figure 6. Lineshape analysis of the fully relaxed spectrum of sample P420. The large dotted Lorentzians centered at 32.4 and 30.5 ppm and the rather wide dotted Lorentzian centered at 32 ppm represent the orthorhombic crystalline and noncrystalline amorphous phases and crystalline−amorphous interphase, respectively. The dashed curve that is almost completely superposed on the experimental spectrum indicates the composite curve of the component Lorentzians. With respect to the weak dashed curves at 39, 34, 28, and 26 ppm, see the legend for Figure 5.

The T_{2C} probes a relatively slower segmental motion with τ_c longer than 10^{-7} s via the spectral density at zero frequency. The T_{2C} as short as 24 μs suggests a high intensity of spectral density at zero frequency. That is, such segmental motion is strongly constrained in the interphase, whereas T_{2C} as long as 410 μs for the amorphous phase indicates that such segmental motion occurs more rapidly with correlation time shorter than 10^{-7} s.

The other resonance lines that are observed at 39, 34, 28, and 26 ppm are assigned to the methine and to the three methylene carbons, respectively, α and β to the methine and in ethyl side groups. They are not pertinent to the present discussion.

Lineshape Analysis of the Spectrum of the Main-Chain Methylene Carbons. From the above analysis, we can conclude that the polyethylene copolymers studied here consist of three phases: the crystalline phase, the noncrystalline amorphous phase, and the crystalline−amorphous interphase. It is evident from the results of the CPTI pulse sequence that the orthorhombic crystalline phase can be fitted to a Lorentzian lineshape with the linewidth of ca. 0.60 ppm centered at 32.4 ppm. The noncrystalline amorphous phase and the crystalline−amorphous interphase can be assumed to be fitted to other Lorentzian lines at 30.5 and 32 ppm by examining the transverse relaxation of their resonances (Figure 4B). An analysis of the lineshape decomposition should then provide the mass fraction of each of the phases. We have attempted to decompose directly the equilibrium spectra shown in Figure 2. However, it was difficult to obtain reproducible results because of the many parameters that need to be determined at once. Therefore, we first decomposed the spectra shown in Figure 4A, which predominantly contain the contribution from the two noncrystalline phases with only a minor contribution from the crystalline phase. The solid curve in Figure 5 gives the 0.5 s saturation−recovery spectrum obatined by pulse sequence II for sample P420. The spectrum contains the contribution from the two noncrystalline phases with T_{1C} of 0.16 s with a negligible contribution from the crystalline phase with a T_{1C} of 0.95 s. This spectrum can be decomposed into two Lorentzians as illustrated by the dotted lines in the figure. This provides a basis for the lineshape analysis of total equilibrium spectrum. That is, with these results, the fully relaxed spectra would be decomposed (by curve fitting) into three components with reproducible results. The result of this decomposition into three Lorentzians is shown in Figure 6. As is seen, the main-chain methylene carbons are well represented by contributions from the orthorhombic crystalline phase, the crystalline−amorphous interphase, and the amorphous phase.

The resonance assigned to the crystal−liquid interfacial region, 32 ppm, is centered very close to that of the orthorhombic crystalline phase of 32.4 ppm. This position is consistent with the interfacial region being comprised of a partially order *trans* chain structure in the longitudinal direction. Disordered units, both *trans* and *gauche*, are also present in relatively small amounts. A similar interpretation was given to the results of a factor analysis of the Raman spectra of linear polyethylene.[35] A third component was found to be present. The spectrum of this component was similar to that of the crystalline phase. However, the peaks were broader and shifted slightly in position. The mass fractions of each of the three phases were obtained by the procedure described for the two samples P16 and P420. The thicknesses of the phases were determined from these mass fractions and the long spacings determined from the small-angle X-ray diffraction analyses. A stacked lamellar structure is assumed for both copolymers in this calculation. The results of this analysis are summarized in Table 2. We note that both the mass fractions and the thicknesses obtained here by the NMR method are in very good agreement with the results previously reported using Raman spectroscopy.[30] The thicknesses of the interphases are estimated to be 13 Å for the two samples, although the molecular weight and the degree of crystallinity differ widely. The results obtained here for the model ethylene copolymers give further support to the concept that there is a quantitatively defined, nonregularly structured interfacial region between the crystalline and amorphous phases.

Partitioning of Methyl Carbons between Different Phases. In our discussion up to now we have tacitly assumed that the ethyl side groups do not enter the lattice, i.e. the crystalline phase remains pure. A central question associated with this class of copolymers is whether the side group enters the lattice and if so under what conditions, i.e. equilibrium or nonequilib-

Table 2. Characterization of Phase Structure: Carbon-13 NMR and Raman Spectroscopy[a]

	crystalline	amorphous	interphase
	Sample P16		
chem shift/ppm	32.4	30.5	32
half-width/Hz	37	88	133
mass fraction (NMR)	0.39	0.43	0.18
mass fraction (Raman)	0.37	0.51	0.12
thickness/Å (NMR)	56	62	13
thickness/Å (Raman)	53	90	10
	Sample P420		
chem shift/ppm	32.4	30.5	32
half-width/Hz	39	78	133
mass fraction (NMR)	0.21	0.61	0.18
mass fraction (Raman)	0.19	0.68	0.13
thickness/Å (NMR)	31	88	13
thickness/Å (Raman)	27	115	10
T_{1C}/s	82, 11, 0.95[b]	0.16	0.16
T_{2C}/ms	0.024	0.41	0.024

[a] NMR data obtained in this work. Raman data obtained previously.[30] [b] The existence of multiple T_{1C}'s for the crystalline phase is a normal finding.[13,16,41]

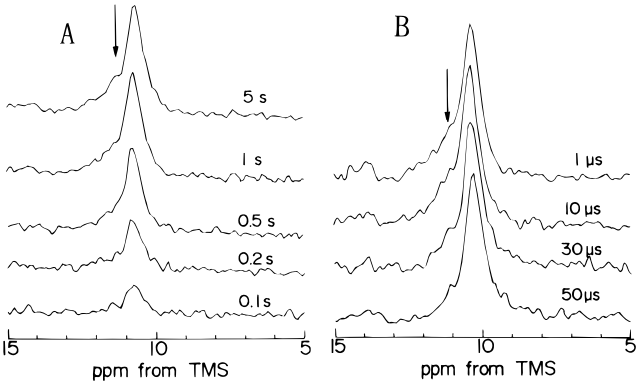

Figure 7. (A) Saturation−recovery spectra in the $1B_2$ carbon range that was obtained with pulse sequence II for sample P16. τ_1 is indicated in each spectrum. (B) Transversely relaxed spectra in the $1B_2$ carbon range that were obtained with pulse sequence III with $\tau_1 = 5$ s for sample P16. τ_t is indicated in each spectrum. In both series of spectra, the arrows indicate a downfield shoulder. (See text.)

rium. A variety of experimental results, involving many different techniques, have made clear that side groups greater than methyl are effectively excluded from the crystal lattice.[32] Among these many techniques, solid-state ^{13}C NMR methods have been used to study this problem.[36−42] Although most of the NMR studies agree with the conclusion cited above, there are some minor disagreements.[36,41,42] Studies with a hydrogenated polybutadiene that contained 1.7 mol % ethyl branches led to the conclusion that a very small proportion, 5−10% of the total branch concentrations, was located within the crystalline region.[41] In a study involving polydisperse, broad composition distribution ethylene−butene copolymers, it was concluded that about 9% of the total branches were located within the lattice.[42] The concentration of ethyl groups entering the lattice that were deduced from these works is admittedly very small. Although it was not the primary objective of the present work, it was opportune to re-examine the problem by analyzing the $1B_2$ carbon resonance (methyl carbon in the ethyl branch) from the spectra obtained in this work. The directly observed spectra of the $1B_2$ carbon are given in Figures 7A and 7B for sample P16. Figure 7A is for the longitudinal recovery with pulse sequence II at progressive times. The transverse relaxation, obtained by means of pulse sequence III, is

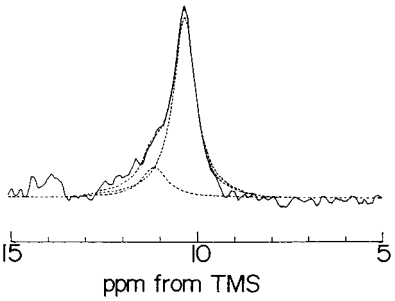

Figure 8. Lineshape of a spectrum in the $1B_2$ carbon range. The spectrum was obtained by the single-pulse sequence with a repetition time of 50 s. (See text.)

given in Figure 7B. In Figure 7A, $1B_2$ resonance, centered at 10.8 ppm, appears within a tenth of a second. It is accompanied by a downfield shoulder at 11.3 ppm, whose position is indicated by the vertical arrow in the figure. Thus, two components contribute to the resonace. They differ in chemical shift but have almost the same T_{1C} of ca. 0.1 s. In the B series spectra, the downfield shoulder quickly disappears and the peak becomes more symmetrical. At 30−50 μs, only the main upfield resonance remains. We can thus conclude that the $1B_2$ carbons are distributed between at least two of the phases with the same T_{1C} of ca. 0.1 s. However, T_{2C} of the downfield resonance is less than 20 μs while that of the upfield resonance is greater than a few milliseconds.

Based on the above analysis, the equilibrium $1B_2$ resonance obtained by the single-pulse sequence, with the repeating time of 50 s, could be decomposed into two Lorentzians. The result of this decomposition is shown in Figure 8.[43] In the resolved spectra, the intensity of the downfield resonance is very small relative to the upfield one. The integrated mass ratio of the downfield resonance to the upfield resonance was estimated to be 1:5. The main upfield resonance can be definitely assigned to the branch methyl carbons in the noncrystalline amorphous phase. The question remains as to the proper phase assignment of the downfield shoulder. Considering the fact that the T_{2C} is as short as 20 μs, this resonance could be assigned to a branch methyl carbon located either in the crystalline region or in the crystalline−amorphous interphase. The concentration of ethyl branches involved is, however, very small, being the order of only 0.44 mol %. We should note here that the T_{1C} of this component is 0.1−0.2 s, and it is the same as in the amorphous phase.

In principle, a methyl carbon with such a short T_{1C} would be assigned to the crystalline phase if the methyl groups were an integral part of the crystal structure. In polypropylene, for example, where this condition is satisfied, the T_{1C} for the methyl carbon in the crystal is much shorter than that for the crystalline methine and methylene ones. The reason for the short T_{1C} is that there is a threefold rotational motion of the methyl group in a frequency range that has an influence on the spin−lattice relaxation time. However, it is not clear whether such an influence would still be manifest if the methyl group is not an inherent part of the crystal structure, as is the case of the copolymers being studied here. Based on the very short T_{1C} and T_{2C} values, the downfield resonance can also be assigned to methyl carbon in the crystalline−amorphous interphase. This assignment would be consistent with other studies involving the location of the ethyl side groups.[32] Since a very large proportion of the methyl groups are located

in the amorphous region, it is not possible, nor reasonable, to assign the downfield resonance completely to the crystalline region. A chain passing between the amorphous and crystalline regions has to traverse the interfacial region. Hence, at a minimum, some of the side groups would have to be located in this region. Based on the present NMR results, one cannot unequivocally distribute the small portion of the total side groups between the two non-liquid-like regions.

VanderHart and co-workers have also studied similar copolymers by ^{13}C NMR solid-state methods.[36,41] The basic spectra that they reported are very similar to those presented here. In their analysis of a hydrogenated polybutadiene sample containing 1.7 mol % branch points (very similar to the one studied here), they found the ratio of the $1B_2$ carbons of the downfield to upfield resonance to be 1:10. Considering the weak intensity of the downfield resonance, this result and that of the present work can be considered to be very similar. However, they assigned the downfield $1B_2$ methyl carbon solely to the crystalline phase because the $T_{1\rho}^{H}$ of 8.2 ms of the $1B_2$ downfield line agreed with that of the $T_{1\rho}^{H}$ of 8.7 ms of the crystalline methylene line. Since only two regions, the crystalline and amorphous phases, were considered in their work,[36,41] it was logical to assign the downfield resonance to the crystalline phase. As was discussed above, with the establishment of a crystal−amorphous interphase and consideration of the T_{1C} and T_{2C}, the downfield resonance can also be assigned to the interphase. Thus, even accepting all of the NMR relaxation data, the existence of the interfacial region precludes a definitive assignment of the methyl branched carbons between the two noncrystalline regions.

Acknowledgment. Support of this work at Florida State University by the National Science Foundation Polymers Program (Grant DMR 94-19508) is gratefully acknowledged.

References and Notes

(1) Flory, P. J. *J. Chem. Phys.* **1949**, *17*, 223.
(2) Flory, P. J. *J. Am. Chem. Soc.* **1962**, *84*, 2857.
(3) Mansfield, M. L. *Macromolecules* **1983**, *16*, 914.
(4) Marqusee, J. A.; Dill, K. A. *Macromolecules* **1986**, *19*, 2420.
(5) Marqusee, J. A. *Macromolecules* **1989**, *22*, 472.
(6) Yoon, D. Y.; Flory, P. J. *Macromolecules* **1984**, *17*, 868.
(7) Flory, P. J.; Yoon, D. Y.; Dill, K. A. *Macromolecules* **1984**, *17*, 862.
(8) Kumar, S. K.; Yoon, D. Y. *Macromolecules* **1989**, *22*, 3458.
(9) Zuniga, I.; Rodrigues, K.; Mattice, W. L. *Macromolecules* **1990**, *23*, 4108.
(10) Dill, K. A.; Naghizadeh, J.; Marqusee, J. A. *Annu. Rev. Phys. Chem.* **1988**, *39*, 425.
(11) Leemaker, F. A. M.; Scheutjens, J. M. H. M.; Gaylord, R. *Polymer* **1984**, *25*, 1577.
(12) Mandelkern, L. *Chemtracts−Macromol. Chem.* **1992**, *3*, 347.
(13) Kitamaru, R.; Horii, F.; Murayama, K. *Macromolcules* **1986**, *19*, 636.
(14) Saito, S.; Moteki, Y.; Nakagawa, M.; Horii, F.; Kitamaru, R. *Macromolecules* **1990**, *23*, 3256.
(15) Hirai, A.; Horii, F.; Kitamaru, R.; Fatou, J. G.; Bello, A. *Macromolecules* **1990**, *23*, 2913.
(16) Axelson, D. E.; Mandelkern, L.; Popli, R.; Mathieu, P. *J. Polym. Sci., Polym. Phys. Ed.* **1983**, *21*, 2319.
(17) Mandelkern, L. *Polym. J.* **1985**, *17*, 337.
(18) Mandelkern, L.; Alamo, R. G.; Kennedy, M. A. *Macromolecules* **1990**, *23*, 4721.
(19) Mandelkern, L.; Alamo, R. G. In *Structure−Property Relations in Polymers: Spectroscopy and Performance*; Urban, M. W., Carver, C. D., Eds.; American Chemical Society: Washington, D.C., 1993; p 157.
(20) Yoon, D. Y.; Flory, P. J. *Polymer* **1977**, *18*, 509.
(21) Yoon, D. Y.; Flory, P. J. *J. Faraday Soc., Discuss. Chem. Soc.* **1979**, *69*, 288.
(22) Yoon, D. Y. *J. Appl. Crystallogr.* **1978**, *11*, 531.
(23) Yoon, D. Y.; Flory, P. J. *Polym. Bull.* **1981**, *4*, 693.
(24) Vonk, C. G. *J. Appl. Crystallogr.* **1973**, *6*, 81.
(25) Santa Cruz, C.; Stribeck, N.; Zachmann, H. G.; Baltá Callejá, F. J. *Macromolcules* **1992**, *24*, 5980.
(26) Stribeck, N.; Alamo, R. G.; Mandelkern, L.; Zachmann, H. G. *Macromolecules* **1995**, *28*, 5029.
(27) Randall, J. C. *J. Polym. Sci., Polym. Phys. Ed.* **1975**, *13*, 1975.
(28) Hsieh, E. T.; Randall, J. C. *Macromolecules* **1982**, *15*, 353.
(29) Hsieh, E. T.; Randall, J. C. *Macromolecules* **1982**, *15*, 1402.
(30) Alamo, R. G.; Chan, E. K. M.; Mandelkern, L.; Voight-Martin, I. G. *Macromolecules* **1992**, *25*, 6381.
(31) Torchia, D. A. *J. Magn. Reson.* **1978**, *30*, 613.
(32) Alamo, R. G.; Mandelkern, L. *Thermochim. Acta* **1994**, *238*, 155.
(33) Howard, P. R.; Crist, B. *J. Polym. Sci., Polym. Phys. Ed.* **1989**, *27*, 2269.
(34) As shown in Table 2, the crystalline phase involves a component with T_{1C} as short as 0.95 s. However, since the mass fraction of this component in the crystalline phase is only 0.14, the contribution from the crystalline phase at $\tau_1 =$ 0.1−1.0 s should be negligible.
(35) Shen, C.; Peacock, A.; Alamo, R.; Vickers, T.; Mandelkern, L.; Mann, C. *Appl. Spectrosc.* **1992**, *46*, 1226.
(36) VanderHart, D. L.; Pérez, E. *Macromolecules* **1986**, *19*, 1902.
(37) Pérez, E.; VanderHart, D. L. *J. Polym. Sci., Polym. Phys. Ed.* **1987**, *25*, 1637.
(38) Lauprêtre, F.; Monnerie, L.; Barthelemy, L.; Vairon, J. P.; Sanzean, A.; Roussel, D. *Polym. Bull.* **1986**, *15*, 159.
(39) McFaddin, D. C.; Russell, K. E.; Kelusky, E. C. *Polym. Commun.* **1986**, *27*, 204.
(40) McFaddin, D. C.; Russell, K. E.; Kelusky, E. C. *Polym. Commun.* **1988**, *29*, 258.
(41) Pérez, E.; VanderHart, D. L.; Crist, B.; Howard, P. R. *Macromolecules* **1987**, *20*, 78.
(42) Pérez, B.; Bello, A.; Pereña, J. M.; Benvavente, R.; Martinez, M. C.; Aquilar, C. *Polymer* **1989**, *30*, 1508.
(43) The weak resonance observed in the range 14−15 ppm can be assigned to the methyl groups of the ends in the main chain. This resonance, however, is not pertinent to our present analysis.

MA951724B